Catechin-7-O-xyloside induces apoptosis via endoplasmic reticulum stress and mitochondrial dysfunction in human non-small cell lung carcinoma H1299 cells

JANG WON YOON[1,6], JONG SUK LEE[2], BYEONG MO KIM[3], JOUNGJWA AHN[4] and KYUNG MI YANG[5]

[1]Department of Food Science and Engineering, Ewha Womans University, Seoul; [2]Gyeonggi Biocenter, Gyeonggi Institute of Science and Technology Promotion, Suwon, Gyeonggi-do, Republic of Korea; [3]Department of Medicine, Beth Israel Deaconess Medical Center, Harvard Medical School, Boston, MA, USA; [4]Department of Food Science and Industry, Jungwon University, Goesan-gun, Chungbuk; [5]Department of Biochemistry and Molecular Biology, Yonsei University, Seoul, Republic of Korea

Received September 12, 2013; Accepted October 14, 2013

DOI: 10.3892/or.2013.2840

Abstract. The medicinal plant *Ulmus davidiana* var. *japonica* has significant potential as a cancer chemoprevention agent. Catechin-7-O-xyloside (C7Ox) was purified from ultrafine *U. davidiana* var. *japonica* ethanol extract. In the present study, we investigated the apoptotic effect of C7Ox in the non-small cell lung cancer (NSCLC) cell line H1299. C7Ox treatment induced cell death and decreased plasma membrane integrity, an event typical of apoptosis. C7Ox-induced apoptosis was associated with the proteolytic activation of caspase-6, cleavage of poly(ADP-ribose) polymerase (PARP) and loss of mitochondrial membrane potential. C7Ox also induced the endoplasmic reticulum (ER) stress-regulated pro-apoptotic transcription factor CHOP. The suppression of CHOP expression significantly decreased C7Ox-induced cell death, LDH leakage and caspase-6 activation. Antitumor effects, evaluated based on protracted tumor regression, were observed when nude-mice bearing H1299 xenografts were treated with C7Ox. C7Ox-induced tumor regression was accompanied by enhanced expression of CHOP mRNA. Our data suggest that C7Ox can trigger mitochondrial-mediated apoptosis, and that ER stress is critical for C7Ox-induced apoptosis in H1299 NSCLC cells.

Correspondence to: Professor Kyung Mi Yang, Department of Biochemistry and Molecular Biology, Yonsei University, Seoul 120-752, Republic of Korea
E-mail: kyungmi_yang@yuhs.ac

Present address: [6]Department of Veterinary Microbiology, College of Veterinary Medicine, Seoul National University, Seoul, Republic of Korea

Key words: Catechin-7-O-xyloside, apoptosis, endoplasmic reticulum stress, C/EBP homologous protein, mitochondrial membrane potential

Introduction

The stem and root bark of *Ulmus davidiana* var. *japonica* (UJ) are Korean herbal medicines which contain many biologically active compounds. Recent studies have shown that UJ has an immunomodulating effect and vasorelaxing activity *in vitro* and *in vivo* (1,2). The major constituents of UJ include flavan-3-ols [(+)-catechin, (+)-catechin 7-O-β-D-apiofuranoside, (+)-catechin 7-O-β-D-xylopyranoside, and (+)-catechin 7-O-β-D-glucopyranoside], triterpene esters, lignan, trihydroxy fatty acid and polysaccharides.

Catechin, one of the major components of the flavan-3-ols, shows efficacy against many cancer types (3-5). Catechin-7-O-glucoside is a flavan-3-ol glycoside formed from catechin and is found in natural traditional drugs such as in the roots of the Chinese peony or is found in foods such as Korean plum-yew (6). However, the molecular mechanism of its selective anticancer role is not clearly understood.

Apoptosis plays a critical role in the development and homeostasis of eukaryotic cells, and impairment of apoptotic function has been associated with several types of human diseases, including cancer and neurodegenerative disorders (7-9). Apoptosis is mediated by the caspases, a conserved family of aspartate-specific cysteine proteases, that can be activated by the mitochondrial pathway (7). Recently, increasing evidence has identified that the apoptotic pathway is linked to the endoplasmic reticulum (ER) stress (10). ER stress is induced by autophagy, oxidative stress and calcium depletion (11-13). The start of ER stress-induced apoptosis occurs through unfolded protein response signaling and involves transcriptional activation of the proapoptotic transcription factor CCAAT/enhancer-binding protein (C/EBP) homologous protein (CHOP) (14). CHOP is a key component in ER stress-mediated apoptosis. For example, CHOP acts to downregulate anti-apoptotic B-cell lymphoma 2 (Bcl-2) protein (15).

Catechin-7-O-xyloside (C7Ox) is a pentose analog of catechin-7-O-glucoside. The cytotoxic effects of C7Ox and the mechanism by which C7Ox exerts its cytotoxic effect remain largely unknown in cancer cells including non-small cell lung

cancer (NSCLC) cells. In the present study, we examined the anticancer effects and molecular mechanisms of C7Ox in H1299 cancer cells. Our results suggest that C7Ox induces apoptosis via the loss of mitochondrial membrane potential and caspase-6 activation, and that the ER stress pathway is important in C7Ox-induced apoptotic cell death in human lung tumor H1299 cells.

Materials and methods

Compound preparation and the biochemical reagents. U. davidiana var. *japonica* (UJ) powder was ground to ultrafine particle size using an herbal medicine pulverizer (Delsa™ Nano; Beckman Coulter Inc., Brea, CA, USA). Catechin-7-O-xyloside (C7Ox) was obtained through purification of an ethanol extract of UJ by using a Sep-Pak cartridge (Waters, Milford, MA, USA). The water-soluble tetrazolium salt (WST)-8 cell proliferation assay kit was obtained from Dojindo Laboratories (Kumamoto, Japan). Lactate dehydrogenase (LDH) cytotoxicity assay and caspase-6 colorimetric assay kits were purchased from Cayman Chemical Co. (Ann Arbor, MI, USA) and Abcam (Cambridge, MA, USA), respectively. The Annexin V/PI apoptosis detection kit was from BD Biosciences (Bedford, MA, USA). Primary antibodies for cleaved-caspase-6, cleaved-poly(ADP-ribose) polymerase (PARP), CHOP and tubulin, and the secondary antibodies were obtained from Cell Signaling Technology (Beverly, MA, USA).

LC-MS/MS analysis. The extract was dissolved in ethanol at a concentration of 10 mg/ml and diluted with 50% ethanol to a final concentration of 2 mg/ml, and 2 μl was analyzed using liquid chromatography followed by tandem mass spectrometry (LC-MS/MS). LC-MS/MS was performed using an LTQ Orbitrap XL ion trap mass spectrometer (Thermo Fisher Scientific, Waltham, MA, USA) equipped with a heated electrospray ionization source. Separation by ultra HPLC (UHPLC) was performed on a Thermo Accela LC system by using an Acquity BEH C18 column (1.7 μm, 2.1 x 150 mm; Waters). Mobile phase A contained water and mobile phase B contained acetonitrile; both contained 0.1% formic acid. Gradient elution at a flow rate of 0.4 ml/min was carried out as follows: 0-1 min with 1-5% B (linear gradient) and 1-10 min with 5-20% B (linear gradient). Full-scan mass spectra were obtained in the negative ion modes at a range *m/z* 100-1000. To identify the structures of the compounds, the data obtained from tandem mass spectrometry (MS/MS) analysis were compared with those from an MS/MS spectral library search (16).

Cell culture. The non-small cell lung cancer (NSCLC) cell line H1299 was purchased from the American Type Culture Collection (ATCC; Manassas, VA, USA). Cells were grown in RPMI-1640 medium containing 10% fetal bovine serum (FBS), 100 U/ml penicillin and 100 μg/ml streptomycin (Gibco-BRL/Life Technologies) in a 5% CO_2 incubator at 37˚C.

Determination of cytotoxicity and plasma membrane integrity. Cell cytotoxicity was assessed by measuring the optical density at 450 nm with a microplate reader (SpectraMax 190®; Molecular Devices Corp., Sunnyvale, CA, USA) 2 h after the addition of 2-(2-methoxy-4-nitrophenyl)-3-(4-nitrophenyl)-5-(2,4-disulfophenyl)-2 H-tetrazolium (WST-8) reagent solution according to the manufacturer's guidelines. Plasma membrane integrity was assessed based on lactate dehydrogenase (LDH) leakage into the culture medium from cells. LDH leakage was determined by measuring the optical density at 490 nm.

Determination of apoptosis by fluorescence-activated cell sorting (FACS) analysis. After C7Ox treatment, cells were harvested and stained with propidium iodide (PI) and Annexin V (BD Biosciences) for 15 min at room temperature in binding buffer and then analyzed using flow cytometry (BD Biosciences). PI and Annexin V emissions were detected in the FL-2 and FL-1 channels, respectively. For each sample, data from 10,000 cells were recorded in list mode on logarithmic scales. Data analysis was conducted using CellQuest software (BD Biosciences).

Assessment of mitochondrial membrane potential. Mitochondrial membrane potential was assessed using the cationic dye JC-1 (5,5',6,6'-tetrachloro-1,1',3,3'-tetraethylbenzimidazolcarbocyanine iodide) according to the manufacturer's instructions (Molecular Probes, Eugene, OR, USA). Images were collected using a Zeiss LSM 510 fluorescence photomicroscope (Carl Zeiss, Oberkochen, Germany). Visualization of JC-1 monomers (green fluorescence) and JC-1 aggregates (red fluorescence) was carried out using filter sets for fluorescein and rhodamine dyes, respectively, and analyzed using ImageJ software.

Detection of caspase-6 activation. A caspase-6 activity assay was conducted using substrates of the color reporter molecule Val-Glu-Ile-Asp-p-nitroaniline (VEID-pNA), which is specific for caspase-6. Briefly, H1299 cells were collected for sampling and lysed on ice by using lysis buffer containing protease inhibitors. Lysates were centrifuged at 13,000 rpm for 10 min at 4˚C, and the supernatant collected was used for the assay. Caspase-6 activity was measured using a microplate reader at 405 nm.

Immunoblotting. Total cell lysate and total tissue protein from lung cancer xenografts of mice were prepared according to a previous study (17). Equal amounts of protein were resolved using sodium dodecyl sulfate-polyacrylamide gel electrophoresis (SDS-PAGE) and transferred to polyvinylidene fluoride (PVDF) membranes (Bio-Rad Laboratories, Hercules, CA, USA). Membranes were probed with antibodies against cleaved caspase-6, poly(ADP-ribose) polymerase (PARP), CHOP, tubulin and secondary antibodies were detected using Pierce ECL-Plus chemiluminescence kit (Thermo Fisher Scientific).

Gene silencing using small interfering RNA (siRNA) transfection. CHOP antisense oligonucleotides (GTCCTGTC TTCAGATGAATT) were synthesized by Genolution Pharmaceuticals, Inc. (Seoul, Korea). Irrelevant scrambled siRNA was used as a control. Cells were transfected with the siRNAs using Lipofectamine reagent (Invitrogen, Carlsbad, CA, USA) according to the manufacturer's instructions.

Xenograft experiment. For the tumor model, H1299 cells ($1x10^6$) were subcutaneously injected into the right flank of female BALB/c nude mice (6 weeks of age) by using a 28-gauge needle. One week later, after the appearance of implanted tumors, the mice were randomly divided into 2 groups: C7Ox group and vehicle group (n=5 mice per group). C7Ox was dissolved in ethanol (EtOH) and diluted with phosphate-buffered saline (PBS) (EtOH:PBS=2:8). C7Ox or vehicle (ie, 20% EtOH in PBS) was intraperitoneally administered once daily for 1 month. Tumor size was calculated by measuring the length and width of the tumor with a caliper. Tumor volume was calculated as follows: Tumor volume (mm^3) = length x $width^2/2$. Next, tumor tissues were collected and frozen at -80˚C until use.

RNA extraction and reverse transcriptase-PCR (RT-PCR). Total RNA from the tumor tissues was extracted using TRIzol reagent (Invitrogen). cDNA was synthesized using the ImProm-II™ reverse transcription system (Promega, Madison, WI, USA) according to the manufacturer's protocol. RT-PCR was performed using a Solgent PCR detection kit following the manufacturer's instructions. Glyceraldehyde 3-phosphate dehydrogenase (GAPDH) was used as an internal control. Primers used included the following: CHOP forward, GACCT GCAAGAGGTCCTG and reverse, CTACTTCCCTGGTCA GGC; GAPDH forward, 5'-GGGCTCATCTGAAGGGTGGT GCTA-3' and reverse, 5'-GTGGACGCTGGGATGATGTTC TGG-3'. The following PCR cycle was used: 1 min of denaturation at 92˚C, 30 sec of annealing at 58˚C and 1 min of extension at 72˚C. PCR was conducted for 28 cycles. PCR products were run on a 0.8% agarose gel and visualized under UV illumination.

Statistical analysis. The data are expressed as the means ± standard error (SE) of at least three independent experiments. Student's t-test was used to assess differences between the two groups. The level of significance was set at P<0.01.

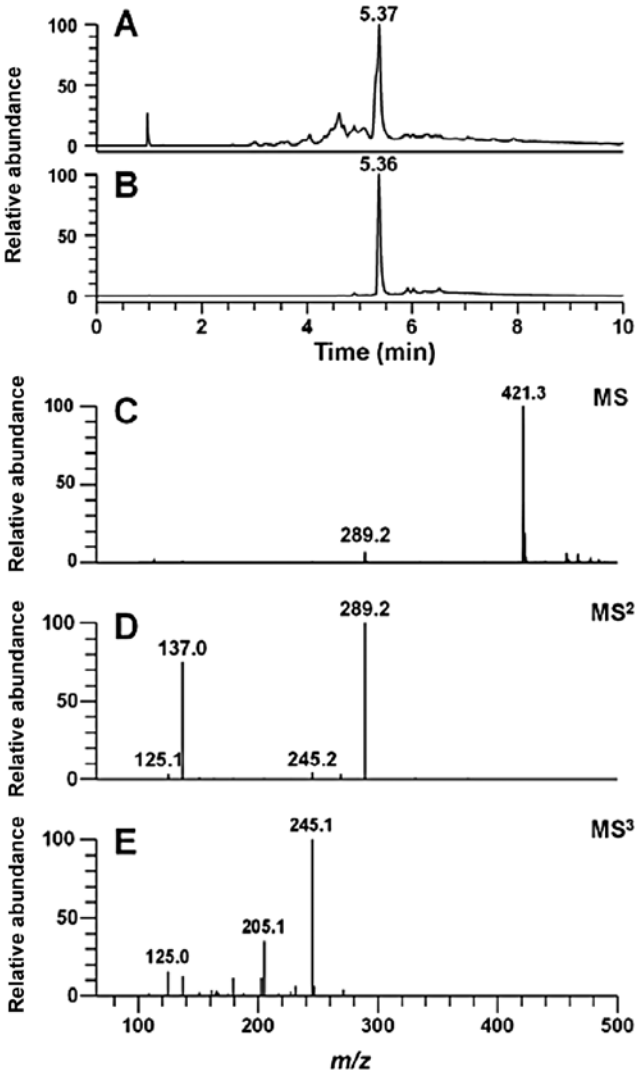

Figure 1. UHPLC-MS analysis results of the major compound. Chromatogram of the (A) extract and (B) purified catechin-7-O-xyloside (C7Ox) at 280 nm, (C) Mass spectrum of the main peak at RT 5.37 min, (D) MS^2 spectrum of *m/z* 421.3 ($[M-H]^-$) and (E) MS^3 spectrum of *m/z* 421.3→*m/z* 289.2.

Results

C7Ox purification from ultrafine U. davidiana var. japonica (UJ) ethanol extract and LC-MS/MS analysis. The 50-mg ethanol extract was loaded on Sep-Pak cartridges and eluted stepwise using 0, 10, 20, 30, 40 and 50% water-ethanol solvent (15 ml each). The 30% fraction was collected and concentrated for the next experiment. The purity of the isolated C7Ox was found to be 87% using ultra high-pressure liquid chromatography (UHPLC) at 280 nm (Fig. 1B). The ultrafine UJ ethanol extract was characterized for its major constituent compounds by simultaneous estimation using negative ion-mode tandem mass analysis (MS^2 and MS^3). The major peak was identified as C7Ox ($[M-H]^-$, *m/z* (mass-to-charge ratio) of 421.3) at RT at 5.37 min (Fig. 1). The sugar moiety was defined using MS^2 fragment ion analysis. Indeed, in the MS^2 spectrum, neutral losses of *m/z* 132 indicated the loss of a pentose. The aglycone structures of MS^3 spectra were identified as catechin by MS/MS spectrum matching (16).

C7Ox induces cell death and increases LDH release. To investigate the cytotoxic effect of C7Ox on cancer cells, we used the WST assay to monitor the survival rate of C7Ox-exposed H1299 cells. Treatment of H1299 cells with C7Ox for 48 h caused dose-dependent decreases in cell survival (P<0.01; Fig. 2A). Next, we investigated whether C7Ox induces LDH release by measuring the activity of LDH released from the cytosol of damaged cells into the medium. As shown in Fig. 2B, LDH release into the culture medium was significantly elevated after C7Ox treatment in H1299 cells when compared with that in the vehicle-treated cells (P<0.01). These results indicated that C7Ox-treated cells underwent postapoptotic necrosis.

C7Ox causes H1299 cell apoptosis. To determine whether this agent induces typical cancer cell apoptosis as well as necrosis, we treated H1299 cells with 400 μM C7Ox for 30 h. After treatment, the cells were harvested and apoptotic cells were examined by FACS analysis using Annexin V/PI staining. As shown in Fig. 2C, C7Ox treatment increased the early apoptotic population (stained by Annexin V only; quadrant 4) from 0.12 to 4.93% as well as the necrotic population (stained by

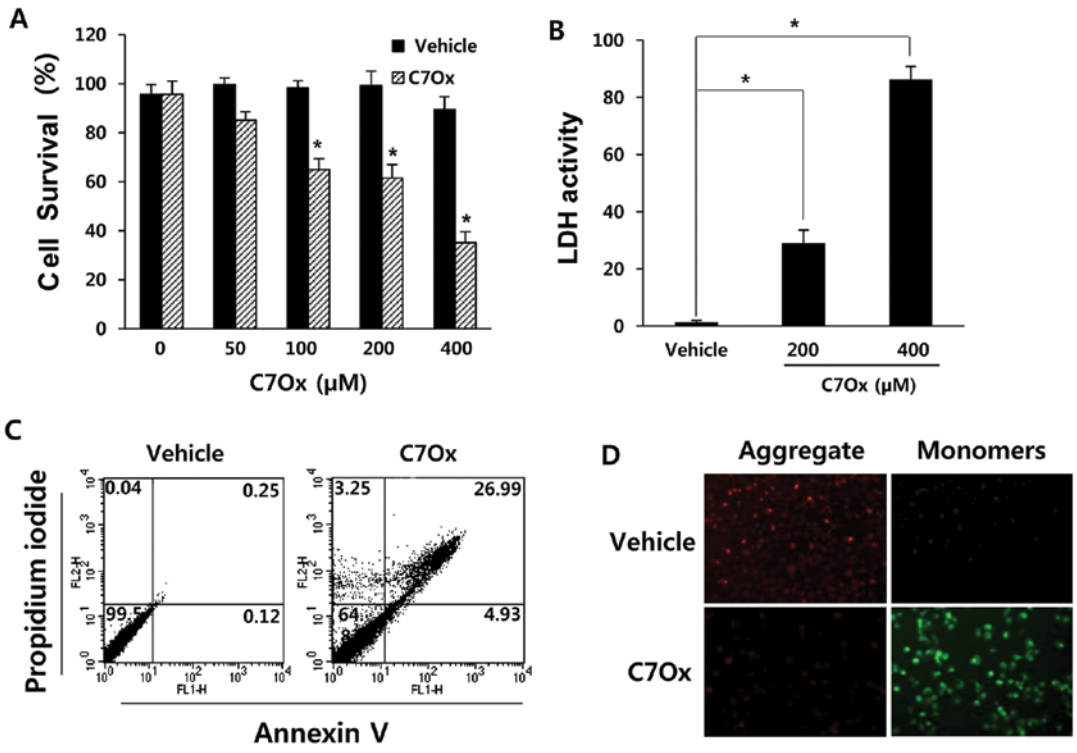

Figure 2. Induction of apoptosis and necrosis of H1299 NSCLC cells following treatment with C7Ox. (A and B) Cells were treated with the indicated concentrations of C7Ox for 48 h for the cell viability assay or 36 h for the LDH assay. (A) Cell viability was detected using a cell counting kit containing WST-8 (*P<0.01 vs. the vehicle control; Student's t-test). (B) LDH release was determined by measuring the conversion of a tetrazolium salt into red-colored formazan (*P<0.01 vs. the vehicle control; Student's t-test). (C and D) Cells were treated with 400 μM C7Ox for 30 h. (C) Apoptotic cells were detected using Annexin V/PI staining. One representative experiment of three is shown. (D) Mitochondrial membrane potential was assayed using the JC-1 probe. Green fluorescence (excitation, 560 nm; emission, 595 nm) indicates JC-1 monomers. Red fluorescence (excitation, 485 nm; emission, 535 nm) indicates JC-1 aggregates. Cells with green fluorescence intensity reflect a decrease in mitochondrial membrane potential. Images are representative of three different experiments.

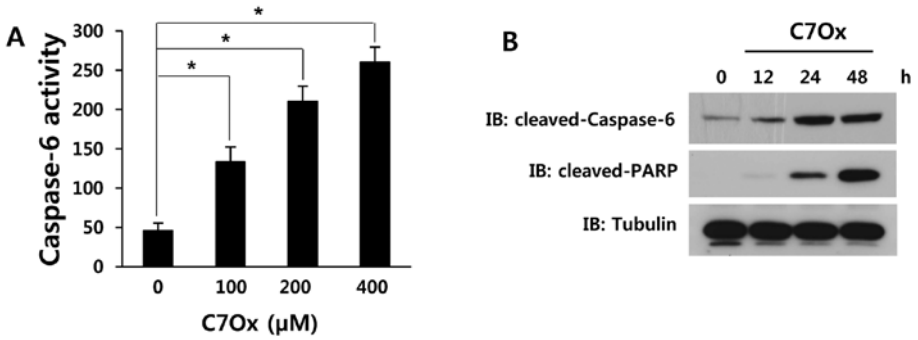

Figure 3. C7Ox induces caspase-6 activation and PARP cleavage in H1299 cells. (A) Cells were treated with the indicated concentrations of C7Ox for 24 h. The change in the activity of caspase-6 was quantitatively measured via the detection of pNA released from the caspase-6 substrate, VEID-pNA (*P<0.01 vs. the vehicle control; Student's t-test). (B) Cells were treated with 400 μM C7Ox for the indicated time periods. Western blotting was used to detect the expression of cleaved caspase-6 and cleaved PARP.

PI only; quadrant 2) from 0.04 to 3.25% or the late apoptotic population (stained by Annexiv V + PI; quadrant 1) from 0.25 to 26.99%. These results indicated that the proportion of apoptotic cells as well as necrotic cells was significantly increased after C7Ox treatment.

C7Ox induces mitochondrial membrane potential collapse. Loss of mitochondrial membrane potential has been linked to the initiation and activation of the apoptotic process (18). To evaluate whether C7Ox triggers mitochondrial injury, the JC-1 probe was used to evaluate the changes in mitochondrial membrane potential during C7Ox treatment. In healthy cells, the dye accumulates in the mitochondria as aggregates with red fluorescence, whereas in apoptotic or dead cells, the dye remains in the cytosol as monomers with green fluorescence. As shown in Fig. 2D, C7Ox-treated cells exhibited a reduction in red emission intensity and a concomitant increase in green emission intensity when compared to vehicle-treated cells. These results indicated that C7Ox treatment induced H1299 cell apoptosis by disrupting the mitochondrial membrane potential.

C7Ox induces proteolytic caspase-6 activation and the cleavage of PARP. Caspase activation and degradation of caspase substrates are key markers of apoptosis (7). We

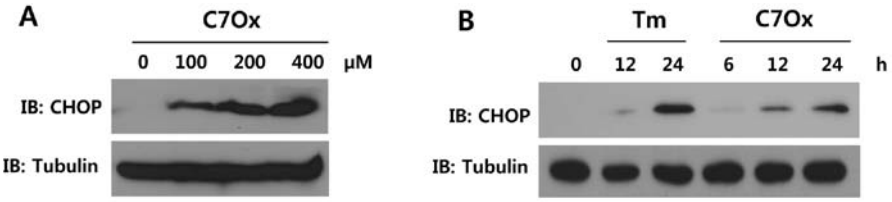

Figure 4. C7Ox induces CHOP expression. Cells were treated with the indicated concentrations of C7Ox for 24 h (A) or treated with 400 μM C7Ox for the indicated time periods (B). The level of CHOP was analyzed by western blotting. Tunicamycin (Tm) (5 μg/ml), a known inducer of ER stress, was used as a positive control.

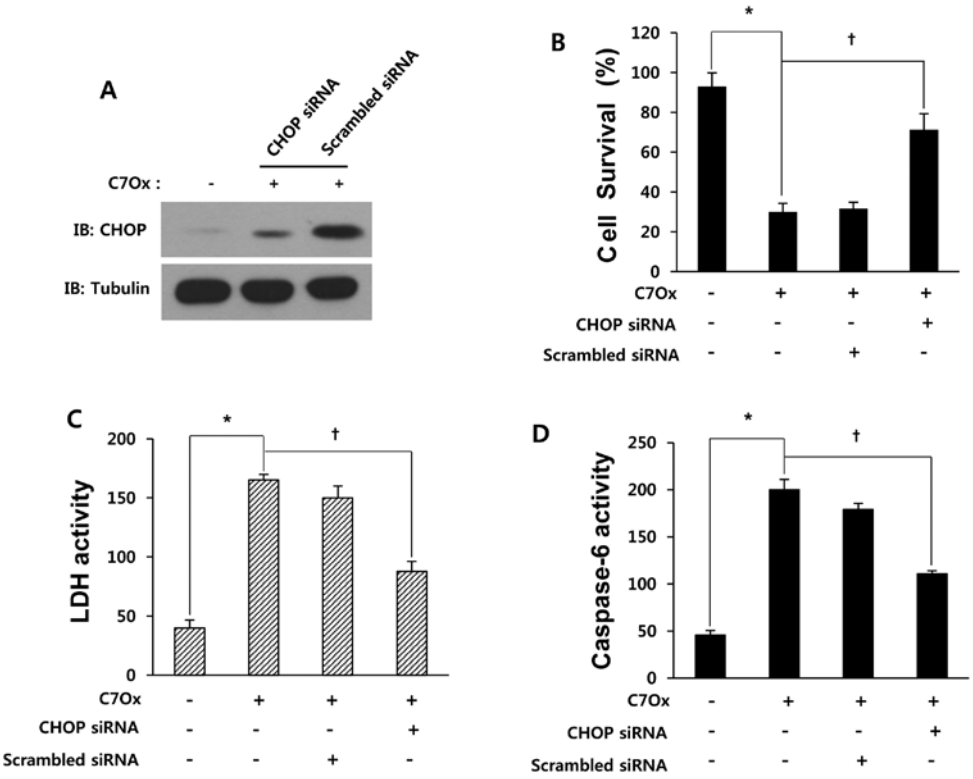

Figure 5. Role of CHOP in C7Ox-induced cytotoxicity and caspase-6 activation in H1299 cells. H1299 cells were transfected with CHOP-specific siRNA or random siRNA control for 30 h and were then treated with 400 μM C7Ox for 24 h (protein assay) or for 48 h (cell viability assay) or for 36 h (LDH activity assay) or for 24 h (caspase-6 activity assay). (A) Knockdown efficiency of CHOP was determined using western blot analysis. The effect of CHOP siRNA on C7Ox-induced (B) inhibition of cell viability, (C) increased LDH release and (D) caspase-6 activation was determined (*P<0.01 vs. the vehicle control, †P<0.01 vs. C7Ox alone; Student's t-test).

confirmed the onset of apoptosis by examining the protease activity using a colorimetric substrate (VEID-pNA) specific for caspase-6. As shown in Fig. 3A, C7Ox activated caspase-6 in a dose-dependent manner (P<0.01). We also examined whether the expression levels of apoptosis-related proteins were affected by C7Ox treatment at various time-points. Western blotting showed that C7Ox significantly increased the cleavages of caspase-6 and PARP proteins in H1299 cells (Fig. 3B).

C7Ox triggers CHOP expression. Apoptotic cell death can be triggered by ER stress, and several pathways have been directly implicated in ER stress-induced apoptosis (10). One of the major components of the ER stress-mediated apoptotic pathway is CHOP expression (19). To investigate whether C7Ox treatment causes ER stress, CHOP expression was measured. Our results showed that C7Ox induced an increase in CHOP expression in a dose- and time-dependent manner (Fig. 4A and B).

Inhibition of CHOP attenuates C7Ox-induced cell death, LDH release and caspase-6 activation. Next, to evaluate the role of CHOP in C7Ox-induced cytotoxicity and apoptosis, we examined the effect of the knockdown of CHOP expression on cell viability, LDH release and caspase-6 activity. As shown in Fig. 5A, C7Ox treatment increased CHOP expression, and CHOP siRNA, but not scrambled siRNA, significantly downregulated CHOP expression providing evidence for the specificity of siRNA inhibition. C7Ox treatment significantly reduced cell viability, increased LDH release and caspase-6 activity, as expected (P<0.01; Fig. 5B-D). However, down-regulation of CHOP expression by CHOP siRNA significantly attenuated C7Ox treatment-induced cell death, LDH release and caspase-6 activation (P<0.01; Fig. 5B-D). C7Ox treatment-

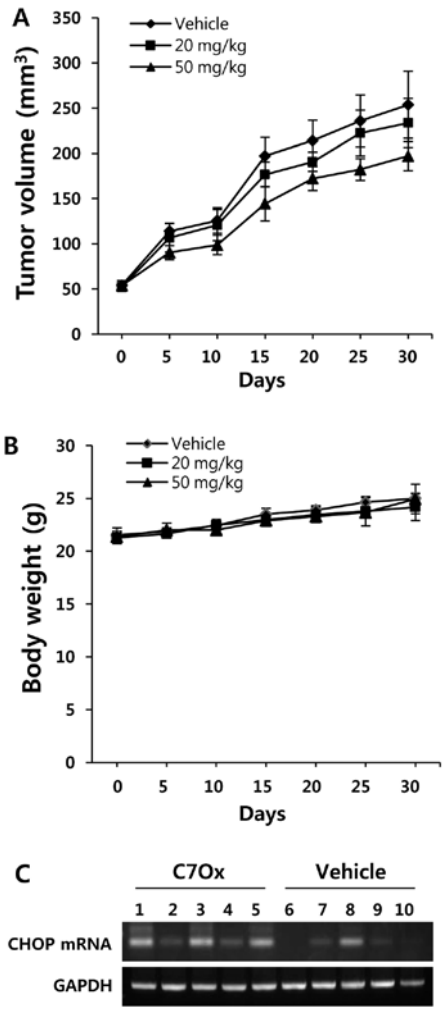

Figure 6. Effect of C7Ox treatment on the growth of H1299 lung cancer xenografts in nude mice. Nude mice bearing subcutaneous H1299 lung carcinoma xenografts (~50 mm^3) were treated with the indicated concentrations of C7Ox or vehicle once daily. Changes in (A) tumor size and (B) body weight in the nude mice bearing tumor xenografts were measured in each treatment group for up to 1 month after treatment. (C) After 1 month of treatment, the expression of CHOP mRNA in both C7Ox-treated and vehicle-treated xenograft tumors was measured using RT-PCR.

induced apoptosis, measured by Annexin V/PI staining, was also attenuated by CHOP siRNA (data not shown). These results suggest that ER stress is responsible for C7Ox-induced apoptotic cell death and caspase-6 activation.

Inhibition of tumor growth in a lung carcinoma xenograft model by C7Ox treatment. To further evaluate the anticancer activity of C7Ox *in vivo*, we treated BALB/c nude mice bearing subcutaneous H1299 cell-derived tumors with either C7Ox (20 mg or 50 mg/kg) or vehicle. Tumor growth was inhibited by C7Ox as compared to the vehicle (Fig. 6A) and there was no apparent change in body weight in the C7Ox-injected animals (Fig. 6B). We also measured the mRNA level of CHOP within the tumor tissue. CHOP mRNA levels were significantly upregulated in the tissues obtained from the C7Ox-treated group when compared with levels obtained from the vehicle-treated group (Fig. 6C). The cleaved caspase-6 protein expression was also upregulated in the tissues obtained from the C7Ox-treated group (data not shown). Our results suggest that C7Ox may be a potential antitumor agent for NSCLC and that ER stress signals are involved in the anticancer activity of C7Ox.

Discussion

We determined whether catechin-7-O-xyloside (C7Ox), the major active constituent purified from the ethanol extract of *U. davidiana* var. *japonica* (UJ), demonstrates anticancer effects and examined its working mechanisms. Although some catechins have antitumor effects (5,20), the effects of catechin derivatives such as catechin-7-O-glucoside or C7Ox on tumors remain unclear. In the present study, we showed that C7Ox induced apoptosis in human H1299 NSCLC cells. We also gained insights into the signaling mechanisms underlying C7Ox-induced apoptosis in this cell line. We monitored the dose response of C7Ox-induced cell death and the elevated release of LDH into the culture medium as indices of cytoplasmic membrane damage and loss of membrane integrity in H1299 cells. The cell viability assay, detection of LDH release, Annexin V/PI staining, caspase-6 activity assay, and western blotting for caspase-6 and PARP showed that C7Ox induced apoptotic cell death as well as post-apoptotic (necrotic) cell death in NSCLC.

Since changes in mitochondrial membrane potential have been directly associated with apoptosis, and a decrease in mitochondrial membrane potential results in the release of cytochrome *c* from impaired mitochondria into the cytosol, resulting in apoptosis (8), we evaluated changes in the mitochondrial membrane potential in NSCLC cells during C7Ox treatment. The decrease in mitochondrial membrane potential, observed using JC-1 dye in the present study, indicated that C7Ox induced apoptosis via a mitochondrial-dependent pathway.

The ER is significantly involved in protein synthesis, maturation and calcium storage in mammalian cells (21). Perturbation of the ER function leads to ER stress, and prolonged ER stress can activate apoptotic pathways in damaged cells (13,15). Therefore, pharmacological interventions that promote cancer cell death through ER stress are attractive options for anticancer therapy (22,23). The transcription factor C/EBP homologous protein (CHOP), an ER stress marker protein, is induced by ER stress and is involved in ER stress-induced apoptosis (19). Treatment of cells with C7Ox was found to cause a dose- and time-dependent increase in the levels of CHOP, indicating that C7Ox can induce ER stress in cancer cells. We also examined the contribution of ER stress to C7Ox-induced apoptotic cell death by using an siRNA that targets CHOP. We found that CHOP siRNA, but not control siRNA, significantly reduced C7Ox-induced cell death, LDH release and caspase-6 activation. CHOP siRNA also suppressed C7Ox-induced apoptosis as assessed by Annexin V/PI staining (data not shown). These findings suggest that C7Ox-induced apoptosis, post-apoptotic necrosis, and caspase-6 activation in human lung cancer cells involve the ER stress pathway.

At a clinically feasible concentration (50 mg/kg), C7Ox significantly delayed H1299 tumor growth in a nude mouse xenograft model, supporting clinical application for anticancer therapy. Notably, CHOP mRNA levels were significantly higher in samples taken from xenografts treated with C7Ox than in samples taken from the vehicle-treated groups.

Caspase-6 protein expression was also higher in xenografts treated with C7Ox (data not shown). Collectively, these data indicated that C7Ox inhibited human lung tumor growth in the mouse xenograft model by triggering ER stress-mediated and caspase-6-mediated apoptosis.

In summary, we demonstrated that C7Ox, a derivative of catechin, induced tumor cell death via both apoptosis and necrosis *in vitro* and *in vivo*. Our findings also suggest that C7Ox triggers ER stress signals and that ER stress molecules such as CHOP contribute to C7Ox-induced apoptotic cell death and caspase-6 activation. Many components from *Ulmus davidiana* var. *japonica* are relatively non-toxic. C7Ox may, therefore, be a potential chemotherapeutic candidate for treating human cancers, including lung cancer.

Acknowledgements

The present study was supported by the Basic Science Research Program through the National Research Foundation of Korea (NRF) funded by the Ministry of Education, Science and Technology (2012R1A1A3003467). J.W.Y. was supported by RP-Grant 2010 of Ewha Womans University.

References

1. Lee EH, Park CW and Jung YJ: Anti-inflammatory and immune-modulating effect of *Ulmus davidiana* var. *japonica* Nakai extract on a macrophage cell line and immune cells in the mouse small intestine. J Ethnopharmacol 146: 608-613, 2013.
2. Cho EJ, Park MS, Kim SS, *et al*: Vasorelaxing activity of *Ulmus davidiana* ethanol extracts in rats: activation of endothelial nitric oxide synthase. Korean J Physiol Pharmacol 15: 339-344, 2011.
3. Li JJ, Gu QH, Li M, Yang HP, Cao LM and Hu CP: Role of Ku70 and Bax in epigallocatechin-3-gallate-induced apoptosis of A549 cells *in vivo*. Oncol Lett 5: 101-106, 2013.
4. Hsu YC and Liou YM: The anti-cancer effects of (-)-epigallocatechin-3-gallate on the signaling pathways associated with membrane receptors in MCF-7 cells. J Cell Physiol 226: 2721-2730, 2011.
5. Singh BN, Shankar S and Srivastava RK: Green tea catechin, epigallocatechin-3-gallate (EGCG): mechanisms, perspectives and clinical applications. Biochem Pharmacol 82: 1807-1821, 2011.
6. Yoon KD, Jeong DG, Hwang YH, Ryu JM and Kim J: Inhibitors of osteoclast differentiation from *cephalotaxus koreana*. J Nat Prod 70: 2029-2032, 2007.
7. Elmore S: Apoptosis: a review of programmed cell death. Toxicol Pathol 35: 495-516, 2007.
8. Lowe SW and Lin AW: Apoptosis in cancer. Carcinogenesis 21: 485-495, 2000.
9. Mattson MP: Apoptosis in neurodegenerative disorders. Nat Rev Mol Cell Biol 1: 120-129, 2000.
10. Gorman AM, Healy SJ, Jäger R and Samali A: Stress management at the ER: regulators of ER stress-induced apoptosis. Pharmacol Ther 134: 306-316, 2012.
11. Kim SJ, Hong EH, Lee BR, *et al*: α-Mangostin reduced ER stress-mediated tumor growth through autophagy activation. Immune Netw 12: 253-260, 2012.
12. Bhandary B, Marahatta A, Kim HR and Chae HJ: An involvement of oxidative stress in endoplasmic reticulum stress and its associated diseases. Int J Mol Sci 14: 434-456, 2012.
13. Mekahli D, Bultynck G, Parys JB, De Smedt H and Missiaen L: Endoplasmic-reticulum calcium depletion and disease. Cold Spring Harb Perspect Biol 3: 1-30, 2011.
14. Zinszner H, Kuroda M, Wang X, *et al*: CHOP is implicated in programmed cell death in response to impaired function of the endoplasmic reticulum. Genes Dev 12: 982-995, 1998.
15. Xu C, Bailly-Maitre B and Reed JC: Endoplasmic reticulum stress: cell life and death decisions. J Clin Invest 115: 2656-2664, 2005.
16. Lee JS, Kim DH, Liu KH, Oh TK and Lee CH: Identification of flavonoids using liquid chromatography with electrospray ionization and ion trap tandem mass spectrometry with an MS/MS library. Rapid Commun Mass Spectrom 19: 3539-3548, 2005.
17. McIntyre A, Patiar S, Wigfield S, *et al*: Carbonic anhydrase IX promotes tumor growth and necrosis in vivo and inhibition enhances anti-VEGF therapy. Clin Cancer Res 18: 3100-3111, 2012.
18. Tsujimoto Y and Shimizu S: Role of the mitochondrial membrane permeability transition in cell death. Apoptosis 12: 835-840, 2007.
19. Szegezdi E, Logue SE, Gorman AM and Samali A: Mediators of endoplasmic reticulum stress-induced apoptosis. EMBO Rep 7: 880-885, 2006.
20. Bharrhan S, Koul A, Chopra K and Rishi P: Catechin suppresses an array of signalling molecules and modulates alcohol-induced endotoxin mediated liver injury in a rat model. PLoS One 6: e20635, 2011.
21. Chakrabarti A, Chen AW and Varner JD: A review of the mammalian unfolded protein response. Biotechnol Bioeng 108: 2777-2793, 2011.
22. Rosati E, Sabatini R, Rampino G, De Falco F, Di Ianni M, Falzetti F, Fettucciari K, Bartoli A, Screpanti I and Marconi P: Novel targets for endoplasmic reticulum stress-induced apoptosis in B-CLL. Blood 116: 2713-2723, 2010.
23. Luo B and Lee AS: The critical roles of endoplasmic reticulum chaperones and unfolded protein response in tumorigenesis and anticancer therapies. Oncogene 32: 805-818, 2013.